
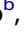











ORIGINAL RESEARCH

 OPEN ACCESS

A BARF1-specific mAb as a new immunotherapeutic tool for the management of EBV-related tumors

Riccardo Turrini ^a, Anna Merlo ^b, Debora Martorelli ^c, Damiana Antonia Faè ^c, Roberta Sommaggio ^d,
Isabella Monia Montagner ^e, Vito Barbieri ^{d,e}, Oriano Marin ^f, Paola Zanovello ^{d,e}, Riccardo Dolcetti ^{c,g,*},
and Antonio Rosato ^{d,e,*}

^aLudwig Center for Cancer Research, University of Lausanne, Lausanne, Switzerland; ^bDepartment of Immunology and Blood Transfusions, San Bortolo Hospital, Vicenza, Italy; ^cCancer Bio-Immunotherapy Unit, Centro di Riferimento Oncologico, IRCCS, National Cancer Institute, Aviano, PN, Italy; ^dDepartment of Surgery, Oncology and Gastroenterology, Oncology and Immunology Section, University of Padova, Padova, Italy; ^eIstituto Oncologico Veneto IOV-IRCCS, Padova, Italy; ^fDepartment of Biomedical Sciences, University of Padova, Padova, Italy; ^gUniversity of Queensland Diamantina Institute, Translational Research Institute, Brisbane, Australia

ABSTRACT

The use of monoclonal antibodies (mAb) for the diagnosis and treatment of malignancies is acquiring an increasing clinical importance, thanks to their specificity, efficacy and relative easiness of use. However, in the context of Epstein-Barr virus (EBV)-related malignancies, only cancers of B-cell origin can benefit from therapeutic mAb targeting specific B-cell lineage antigens. To overcome this limitation, we generated a new mAb specific for BARF1, an EBV-encoded protein with transforming and immune-modulating properties. BARF1 is expressed as a latent protein in nasopharyngeal (NPC) and gastric carcinoma (GC), and also in neoplastic B cells mainly upon lytic cycle induction, thus representing a potential target for all EBV-related malignancies. Considering that BARF1 is largely but not exclusively secreted, the BARF1 mAb was selected on the basis of its ability to bind a domain of the protein retained at the cell surface of tumor cells. *In vitro*, the newly generated mAb recognized the target molecule in its native conformation, and was highly effective in mediating both ADCC and CDC against BARF1-positive tumor cells. *In vivo*, biodistribution analysis in mice engrafted with BARF1-positive and -negative tumor cells confirmed its high specificity for the target. More importantly, the mAb disclosed a relevant antitumor potential in preclinical models of NPC and lymphoma, as evaluated in terms of both reduction of tumor masses and long-term survival. Taken together, these data not only confirm BARF1 as a promising target for immunotherapeutic interventions, but also pave the way for a successful translation of this new mAb to the clinical use.

Abbreviations: ADCC, antibody-dependent cell-mediated cytotoxicity; CDC, complement-dependent cytotoxicity; CFA, complete Freud adjuvant; CTLs, cytotoxic T lymphocytes; EBV, Epstein-Barr virus; ELISA, enzyme-linked immunosorbent assay; hCSF-1, human colony-stimulating factor; IFA, incomplete Freud adjuvant; IFN- α , interferon- α ; LV-LUX, luciferase-encoding lentiviral vector; mAbs, monoclonal antibodies; NK, natural killer; NPC, nasopharyngeal carcinoma; PEG, polyethyleneglycol; PTLD, post-transplant lymphoproliferative disease; PVDF, polyvinylidene fluoride; RAG, recombination-activating gene; SCID, severe combined immunodeficiency

ARTICLE HISTORY

Received 17 November 2016
Revised 3 March 2017
Accepted 3 March 2017

KEYWORDS



ADCC; BARF1; CDC; Epstein-Barr virus; immunotherapy; monoclonal antibody

Introduction

The Epstein-Barr virus (EBV) is a γ -herpesvirus associated with the development of both lymphoid and epithelial malignancies, each characterized by a distinct pattern of viral protein expression.¹ Since viral proteins are expressed almost exclusively in malignant cells, they represent an ideal target for immunotherapeutic strategies, as demonstrated by the success of EBV-specific adoptive T-cell therapy, especially against post-transplant lymphoproliferative disease (PTLD) in which the full array of latent EBV proteins is expressed.² However, albeit highly heterogeneous, the infused cytotoxic T lymphocytes

(CTLs) are able to target only a few subdominant EBV antigens, such as LMP-1 and LMP-2, thus accounting for the less satisfactory results obtained against tumors characterized by a restricted pattern of latent protein expression.²

One of these “neglected” proteins is represented by BARF1, which recently proved to be a very attractive target for improving adoptive immunotherapy of nasopharyngeal carcinoma (NPC).^{3,4} Unlike classic EBV tumor-associated latency proteins, BARF1 is mainly considered an early lytic protein in a normal B-cell background, whereas it is consistently expressed during latency in EBV-related NPC and gastric carcinoma

CONTACT Antonio Rosato  antonio.rosato@unipd.it  Department of Surgery, Oncology and Gastroenterology, Oncology and Immunology Section, University of Padova, Via Gattamelata 64, 35128 Padova, Italy.

*These are co-senior authors to this work.

Published with license by Taylor & Francis Group, LLC © Riccardo Turrini, Anna Merlo, Debora Martorelli, Damiana Antonia Faè, Roberta Sommaggio, Isabella Monia Montagner, Vito Barbieri, Oriano Marin, Paola Zanovello, Riccardo Dolcetti, and Antonio Rosato.

This is an Open Access article distributed under the terms of the Creative Commons Attribution-NonCommercial-NoDerivatives License (<http://creativecommons.org/licenses/by-nc-nd/4.0/>), which permits non-commercial re-use, distribution, and reproduction in any medium, provided the original work is properly cited, and is not altered, transformed, or built upon in any way.

(GC).⁵⁻⁷ Whether BARF1 is also expressed in EBV latently infected lymphoma cells, remains to be elucidated.

BARF1 is a 221 amino acid (aa) transmembrane protein expressed at the surface of EBV-infected cells, although the extracellular domain can be cleaved after the first 20 aa and shed, thus exerting its pleiotropic functions both in *cis* and in *trans*. Indeed, BARF1 was shown to immortalize simian and human epithelial cells,^{8,9} and human B lymphocytes.¹⁰ Importantly, mouse fibroblasts immortalized upon BARF1 transfection-induced tumors when injected in newborn rodents.¹¹ Ectopic expression of BARF1 or treatment of cells with its secreted form were shown to promote the growth of different cell types, including mouse fibroblasts, human B cells, primary monkey and human epithelial cells.¹² Interestingly, this autocrine/paracrine cell growth promotion can be blocked by anti-BARF1 antibodies.^{13,14}

Immortalizing and transforming properties of BARF1 are dependent on the activation of various intracellular signaling pathways including c-myc activation,¹⁰ induction of cyclin-D expression,¹⁵ upregulation of the anti-apoptotic molecule Bcl-2,¹⁶ and SMAD4 suppression through NF- κ B-mediated miR-146a upregulation.¹⁷ In addition, due to a limited homology with the human colony-stimulating factor 1 (hCSF1) receptor, BARF1 may act as an allosteric decoy receptor for hCSF1,¹⁸ thereby interfering with human monocyte and macrophage differentiation and activity *via* down-modulation of surface marker expression, reduction of cell viability¹⁹ and IFN α release.²⁰ By manipulating monocyte and macrophage physiology, BARF1 may therefore exert an immune-modulating role thus contributing to render the tumor invisible to the immune system.

On these grounds, BARF1 can be regarded as an ideal candidate for a monoclonal antibody (mAb) therapy, both in its membrane-associated and shed forms. We therefore aimed at developing a novel BARF1-specific mAb for passive immunotherapy of EBV-related malignancies. In this regard, BARF1-specific polyclonal and monoclonal antibodies described thus far have not been tested for immunotherapeutic approaches. Here, we describe the successful generation of a BARF1-specific monoclonal antibody and its *in vitro* and *in vivo* functional characterization. The mAb proved to be effective in complement-dependent cytotoxicity (CDC) and antibody-dependent cell-mediated cytotoxicity (ADCC) assays against a panel of BARF1-positive tumor cells. Moreover, biodistribution analysis exploiting *in vivo* fluorescence imaging demonstrated its specific targeting to EBV-related tumor masses. In immunotherapy experiments involving BARF1-positive NPC and lymphoma preclinical models, the mAb restrained tumor growth and improved long-term survival of treated animals.

Taken together, these data corroborate the role of BARF1 as a novel EBV-specific tumor antigen suitable for immunotherapeutic approaches, and support the concept that anti-BARF1 mAb can be regarded as promising new tools for the treatment of most EBV-related malignancies.

Results

Immunization and monoclonal antibody production

Conventional BALB/c mice were immunized with KLH-conjugated peptides (BARF1₂₀₁₋₂₂₁, BARF1₁₀₄₋₁₂₀ and BARF1₂₈₋₃₈;

Fig. 1A) according to a routine schedule, and sera were collected and analyzed by ELISA test. All the peptides used for immunization induced strong antibody production that resulted in elevated absorbance values even at very high sera dilutions (data not shown), thus demonstrating the immunogenicity of the KLH-conjugated peptides. Since BARF1 is expressed on the surface of EBV-infected cells,²¹ we decided to use GRANTA-519 cell line, a human mantle lymphoma cell line expressing EBV and BARF1 mRNA,³ to screen mouse sera by flow cytometry. After the first round of three immunizations, GRANTA-519 resulted negative, thus requiring additional immunizations of mice before a detectable signal was evident. Interestingly, peptide-specific immunoglobulin titres, as assessed by ELISA, remained almost at the same maximal levels, indicating that antibody titres did not increase but improved in terms of intrinsic affinity and ability to recognize naturally folded epitopes that are physiologically presented on the cell surface. After hybridoma generation from the best reactive mouse, the same ELISA and flow cytometry-based screenings were also adopted to analyze the derived clones, ultimately leading to the selection of a single clone (3D4, an IgG2a-secreting hybridoma derived from a mouse immunized with peptide BARF1₂₈₋₃₈) that was chosen for subsequent analyses.

As a first proof of BARF1 target recognition, the 3D4 antibody was used in a Dot Blot assay. All the peptides used for immunization, and two 4-aa overlapping peptides derived from peptide BARF1₂₈₋₃₈, were spotted on PVDF to identify the epitope recognized by anti-BARF1 antibody. Dot blot analysis revealed that the 3D4 mAb did not recognize unrelated peptides (BARF1₂₀₁₋₂₂₁ and BARF1₁₀₄₋₁₂₀), while the BARF1₂₈₋₃₈ peptide was positively stained. Of the two additional peptides derived from peptide BARF1₂₈₋₃₈, only peptide BARF1₂₈₋₃₅ was recognized by the 3D4 mAb, thus indicating that the recognized epitope resides within its sequence (Fig. 1A). BLAST analysis revealed that the peptide sequence is specific for the BARF1 protein and for the human colony-stimulating factor 1 receptor (hCSF-1 receptor), which is known to share homology with BARF1 protein.²²

The 3D4 mAb specifically identifies BARF1 on tumor cell lines of different histotypes

The anti-BARF1 3D4 mAb stained EBV⁺BARF1⁺ tumor cell lines belonging to different histotypes, whereas EBV-negative and BARF1-negative cells were not stained (Fig. 1B). Notably, the EBV⁺ Raji cell line was not recognized by the 3D4 mAb, consistently with its negativity for BARF1 expression due to a deletion in the corresponding gene within the EBV genome,²³ thus further supporting the specificity of the mAb. The differences in the mean fluorescence intensity observed among the positive cells are likely to be ascribed to the differential expression of BARF1. Indeed, few information is available about BARF1 expression levels on the cell surface, so that we may expect a differential protein expression on different cell lines, or on the same cell line but at different culture stages (in fresh medium rather than in an exhausted, acidified medium). Moreover, cleavage of the extracellular BARF1 domain has

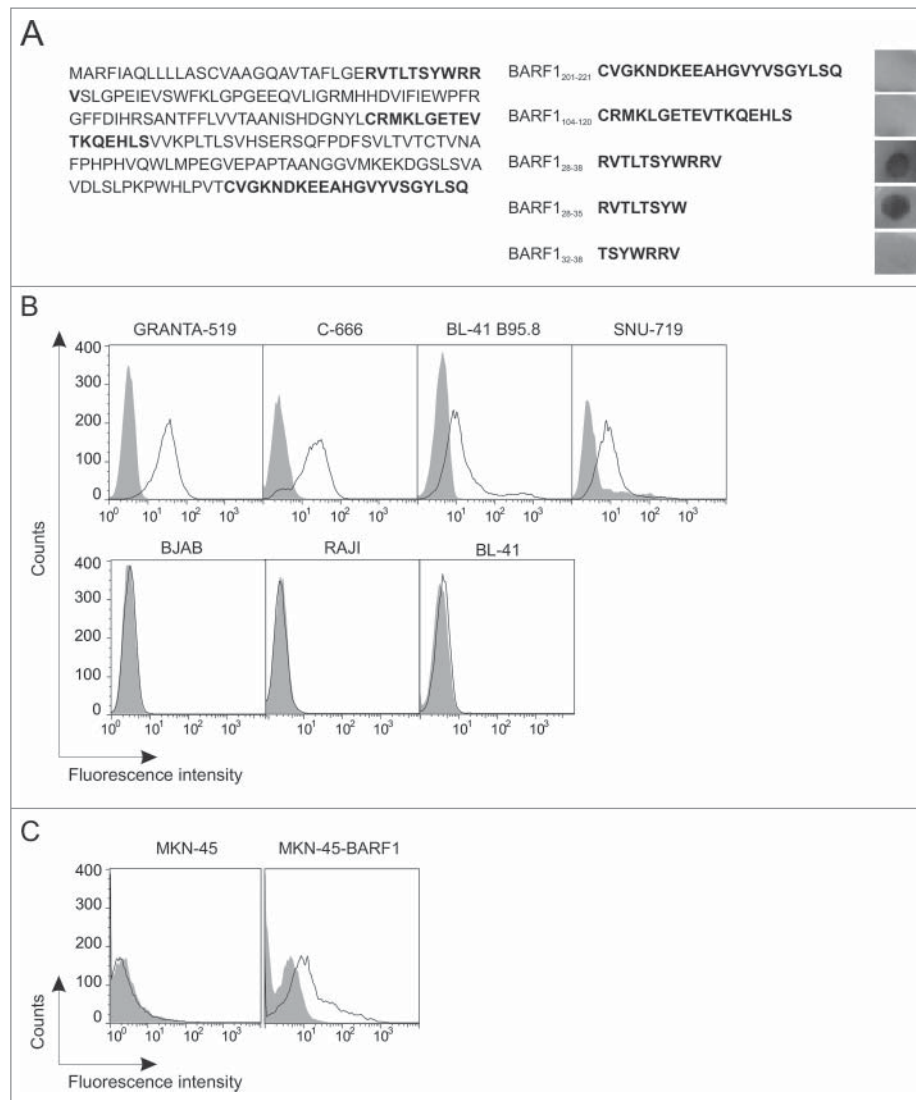


Figure 1. BАРF1 mAb generation and characterization. (A) Left: BАРF1 sequence (NCBI Reference Sequence: YP_401719.1) and derived peptides. Right: dot Blot analysis. Peptides BАРF1₂₀₁₋₂₂₁, BАРF1₁₀₄₋₁₂₀ and BАРF1₂₈₋₃₈ are highlighted in the amino acidic sequence of the whole protein. A positive staining was detected only on peptide BАРF1₂₈₋₃₈ and the derived BАРF1₂₈₋₃₅, thus identifying the minimal epitope of the selected antigen. (B) Flow cytometry analysis of BАРF1 expression by GRANTA-519, C-666, BL-41 B95.8, SNU-719, BJAB, RAJI and BL-41 cell lines. (C) Flow cytometry analysis of BАРF1 expression by MKN-45 cells before and after transduction with a BАРF1-coding retrovirus.

been reported, even though the cleavage rate is still to be elucidated.²⁴

To further confirm the specificity of the antibody for its target, we ectopically expressed BАРF1 in the EBV-negative MKN-45 GC cell line. As shown in Fig. 1C, the 3D4 mAb clearly labeled BАРF1-transduced MKN-45 cell line, whereas parental cells showed only background staining, thus demonstrating the fine specificity of the mAb.

The 3D4 mAb mediates both CDC and ADCC *in vitro*

Complement-dependent cytotoxicity (CDC) was assessed in a standard chromium release assay, using both EBV-positive and -negative cell lines as target cells. As shown in Fig. 2A, EBV-positive cell lines (GRANTA-519, C-666, BL-41 B95.8 and SNU-719) were specifically lysed when exposed to both 3D4 mAb and complement; in the same experimental conditions, the EBV-negative BL-41 cell line showed only a background level of lysis.

ADCC was performed using Calcein AM on the same panel of EBV-positive and -negative cells already used in CDC, with PBMC from healthy donors serving as effector cells. As shown in Fig. 2B, the 3D4 mAb was able to specifically mediate ADCC of BАРF1⁺ target cells. The highest level of lysis of BАРF1-positive target cells was obtained with 20 μ g/mL of the 3D4 mAb at an effector:target ratio of 300. As evaluated by flow cytometry, the percentage of CD16⁺CD56⁺ NK cells in PBMC was in the range of 12–15% of the total population (data not shown).

The 3D4 mAb specifically targets BАРF1-positive tumors *in vivo*

Biodistribution analysis and *in vivo* targeting capacity of the mAb were assessed by tracking the fluorescence signal of Alexa-680-conjugated anti-BАРF1 antibody, following injection in mice grafted with EBV-positive (C-666) or -negative

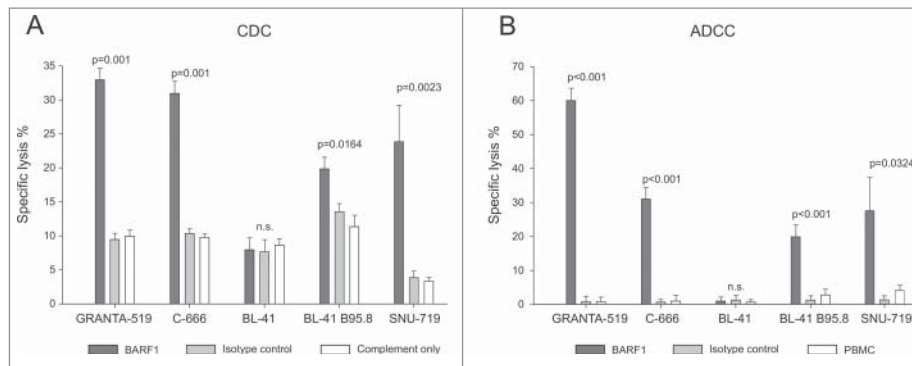


Figure 2. BARF1 mAb *in vitro* functional activity. (A) CDC. Specific lysis of EBV-positive (GRANTA-519, C-666, BL-41 B95.8 and SNU-719) and -negative (BL-41) cell lines after exposure to the 3D4 anti-BARF1 mAb and Complement. The isotype control and Complement alone were used as negative controls. (B) ADCC. Specific lysis of EBV-positive and EBV-negative cell lines after exposure to the 3D4 anti-BARF1 mAb and human PBMC from healthy donors. The isotype control and PBMC alone were used as negative controls. Data from three independent experiments were analyzed by Student's *t*-test and data are reported in the figure as mean \pm SD.

(MKN-45) cell lines at two distinct sites. The analysis was performed daily for 1 week, and the values of fluorescence intensity were recorded for the two tumor masses. As previously reported,²⁵ a whole intact mouse mAb requires at least 3 d to accumulate differentially at the site of antigen-expressing tumor; indeed, by day 3, the 3D4 mAb showed a markedly higher accumulation at the site of BARF1⁺ C-666 tumor mass, as compared with the EBV-negative counterpart (Fig. 3A). As an additional proof of specificity, the same biodistribution analysis was performed in mice injected at two distinct sites with untransduced or BARF1-transduced MKN-45 cells. Again, a strong and highly

specific signal could be progressively detected only from the BARF1⁺ MKN-45 cancer mass (Fig. 3B), thus indicating that the 3D4 mAb is specific for the BARF1 protein and capable of recognizing the viral antigen also *in vivo*.

Administration of 3D4 mAb to tumor-bearing mice restrains primitive cancer growth and reduces metastatic spreading

Tumor cell lines of different histotypes were injected in SCID mice either s.c. or i.v. to evaluate the therapeutic activity of anti-BARF1 antibody in tumor mouse models. In the C-666

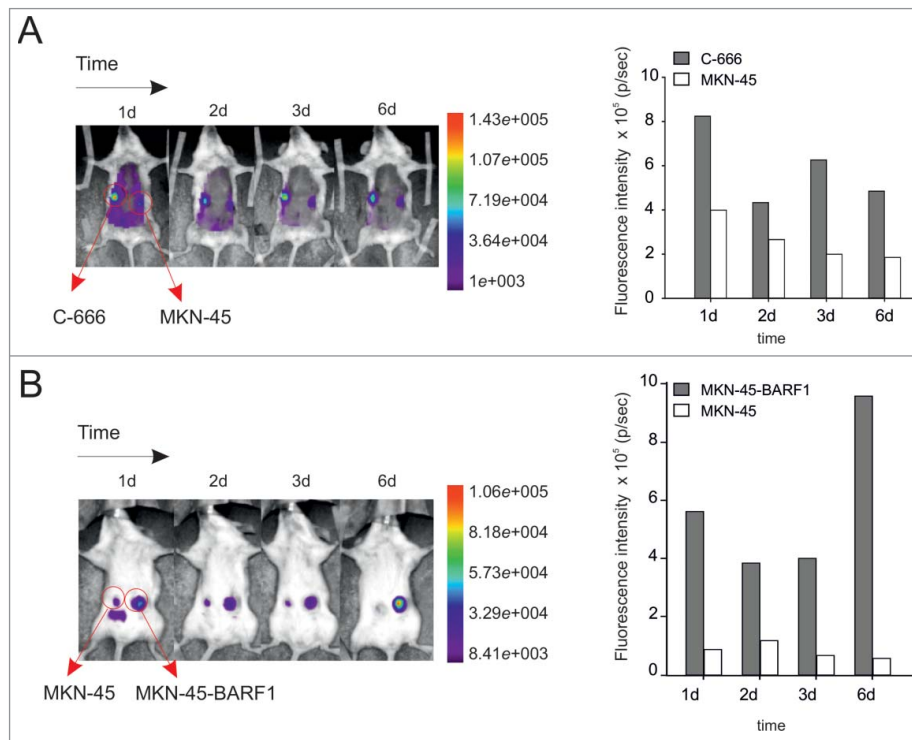


Figure 3. BARF1 mAb *in vivo* biodistribution by fluorescence analysis. Left panels show a representative SCID mouse injected s.c. on one flank with C-666 NPC cells and on the opposite one with MKN-45 GC cells (A), or with MKN-45 GC cells and BARF1-transduced MKN-45 GC cells (B), at two distinct sites. After i.v. injection of Alexa680-conjugated anti-BARF1 mAb, the fluorescence was analyzed at different time points thereafter. Right panels show the histogram representation of fluorescence intensity (p/sec). The experiment was repeated twice with consistent results.

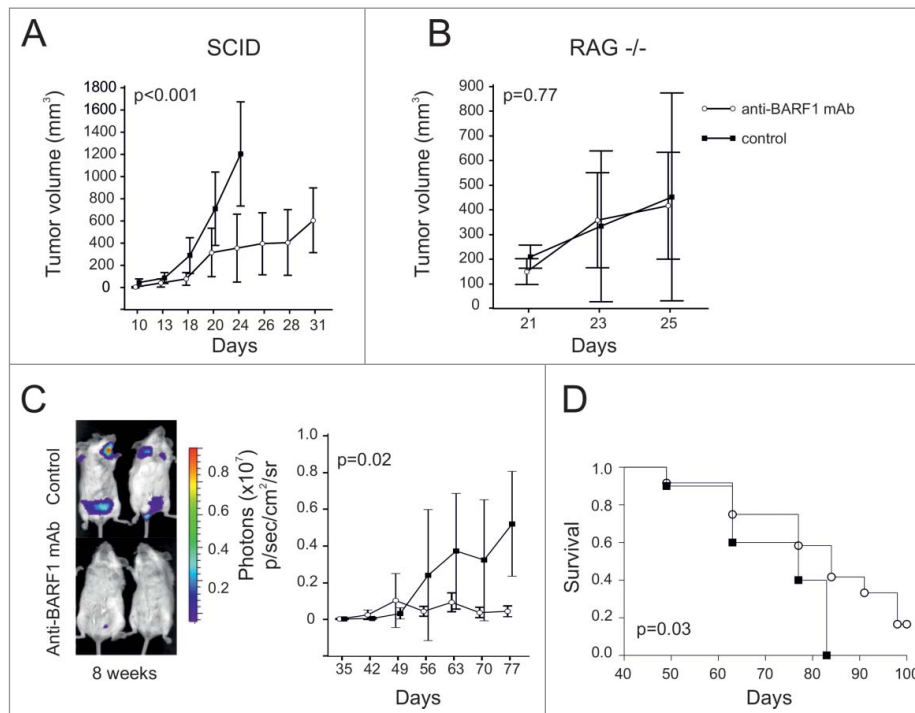


Figure 4. Therapeutic activity of BARF1 mAb in a NPC mouse model. On day 0, (A) SCID mice and (B) RAG^{-/-} γ -chain^{-/-} mice were injected s.c. with 5×10^6 C-666 cells. Mab-treated mice ($n = 9$) received a total amount of 1 mg of the 3D4 anti-BARF1 antibody (white circles) starting at day 10 (palpable tumor), while control animals ($n = 5$) were injected with PBS only (black squares). The therapy with the antibody significantly delayed the tumor growth ($p < 0.001$) in (A), while no effect was observable in (B) ($p = 0.77$). (C) Bioluminescence analysis of SCID mice injected i.v. at day 0 with 3×10^6 C-666-LUX cells, and receiving anti-BARF1 mAb (1 mg) treatment according to the previous schedule. Left panel refers to two representative treated and control mice 8 weeks after cell injection. Right graph shows cumulative BLI data from all animals (control = 10 mice, treated = 12 mice) at different time points of analysis. Mab treatment significantly reduced tumor growth ($p = 0.02$). (D) Kaplan-Meier survival curves of mice reported in (C): anti-BARF1 mAb therapy significantly increased survival ($p = 0.03$).

cell s.c. model, the 3D4 mAb treatment strongly decreased primary tumor growth ($p < 0.001$; Fig. 4A), relative to the control. Conversely, in mice injected s.c. with the EBV⁺ BARF1-negative Raji cells, the treatment did not produce any therapeutic effect (data not shown), consistent with *in vitro* results.

The C-666 cell line was also injected s.c. in RAG^{-/-} γ -chain^{-/-} mice (which lack functional B, T and NK cells), but no difference in cancer growth was observed between treated and control group ($p = 0.77$; Fig. 4B), thus suggesting that the main effector mechanism of the 3D4 mAb *in vivo* likely relies on NK cells and ADCC.

To assess the systemic and metastatic behavior of the same cell line upon i.v. injection, we took advantage of a bioluminescent model based on C-666 cells transduced with a luciferase reporter gene. Under these experimental conditions, treatment with the 3D4 mAb provided further strong evidence of therapeutic activity, as tumor growth was heavily delayed in treated mice as compared with control animals and the metastatic progression almost completely abrogated ($p = 0.02$; Fig. 4C). Moreover, mAb activity impacted on survival that significantly improved in treated vs. control mice ($p = 0.03$; Fig. 4D).

A similar approach was also adopted to assess the therapeutic effects of 3D4 mAb in a different tumor model represented by the s.c. or systemic injection of the GRANTA-519 cell line. Upon s.c. inoculation, tumor growth was fast in the control group, while appeared significantly reduced in mAb-treated mice ($p < 0.001$; Fig. 5A). As for the C-666 model, when performed in RAG^{-/-} γ -chain^{-/-} mice the same assay did not bring about any significant difference in GRANTA-519 tumor

growth ($p = 0.14$; Fig. 5B), thus underlying the importance of ADCC as a functional mechanism of anti-BARF1 antibody. When luciferase-transduced GRANTA-519 cells were administered i.v., the treatment with the anti-BARF1 mAb again dramatically restrained tumor growth and dissemination ($p = 0.03$, Fig. 5C), and led to an improved survival ($p = 0.002$; Fig. 5D).

Discussion

The dual tropism of the oncogenic EBV for B lymphocytes and epithelial cells reflects on the development of both lymphomas and carcinomas. Among them, only B-cell lymphomas can take advantage of mAb therapy, being successfully treated by targeting some lineage-specific markers such as CD20, CD22, CD30, CD37, CD52, and CD79a.²⁶ However, these antibodies do not discriminate between normal and malignant cells, thus leading to the possible development of cytopenias and hypogammaglobulinemia.²⁶ In addition, a significant percentage of patients develops resistance.²⁶ To overcome these limitations, we identified the viral protein BARF1 as a specific and shared target for a mAb therapy against potentially all EBV-related tumors, since it is expressed as latency protein in EBV-driven carcinomas as well as in lymphomas, at least as an early lytic protein in these latter tumors. Further studies are, however, required to conclusively assess the expression of BARF1 protein in EBV latently infected lymphoma cells. Moreover, BARF1 was recently demonstrated to be a good target for cell-based immunotherapeutic strategies. Despite the fact that this protein is considered poorly

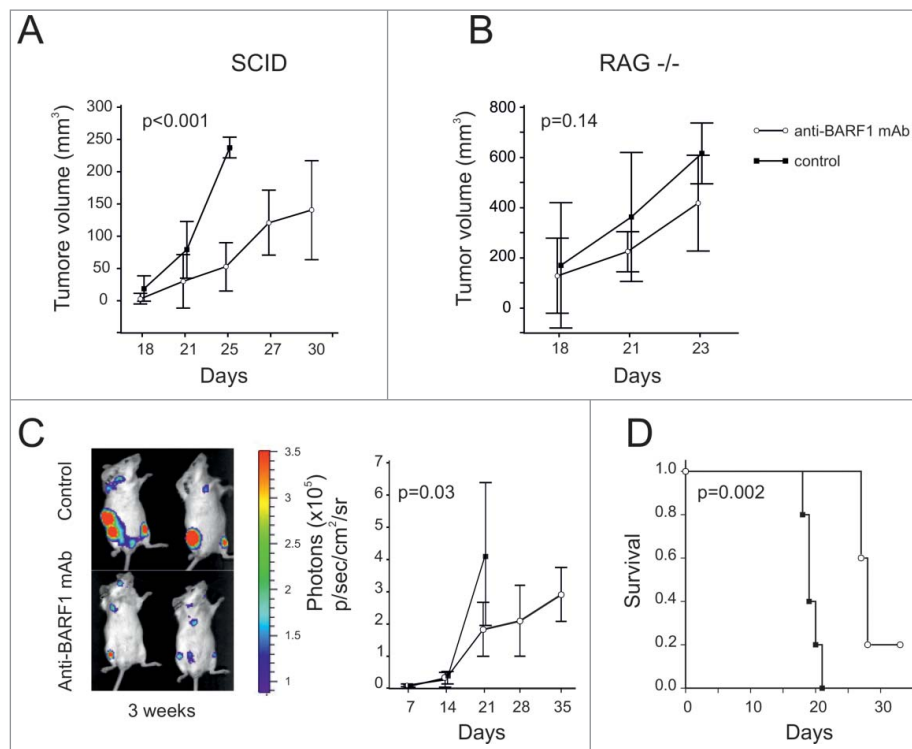


Figure 5. Therapeutic activity of BARF1 mAb in a lymphoma mouse model. On day 0, (A) SCID mice and (B) RAG^{-/-} γ -chain^{-/-} mice were injected s.c. with 5×10^6 GRANTA-519 cells. Mab-treated mice ($n = 13$) received a total amount of 1 mg of the 3D4 anti-BARF1 antibody (white circles) starting at day 14 (palpable tumor), while control animals ($n = 9$) were injected with PBS only (black squares). The therapy with the antibody significantly delayed the tumor growth ($p < 0.001$) in (A), while no effect was observable in (B) ($p = 0.14$). (C) Bioluminescence analysis of SCID mice injected i.v. at day 0 with 3×10^6 GRANTA-519-LUX cells, and receiving anti-BARF1 mAb (1 mg) treatment according to the previous schedule. Left panel refers to two representative treated and control mice 3 weeks after cell injection. Right graph shows cumulative BLI data from all animals (10 mice/group) at different time points of analysis. Mab treatment significantly reduced tumor growth ($p = 0.03$). (D) Kaplan-Meier survival curves of mice reported in (C): anti-BARF1 mAb therapy significantly increased survival ($p = 0.002$).

immunogenic, nevertheless both humoral and cellular immune responses have been described in NPC patients.^{3,27} Of note, EBV-specific CTL responses appeared to be protective to some extent in a particular cohort of NPC patients, where the HLA molecules that efficiently present CTL epitopes turned out to be significantly under-represented as compared with the general population.²⁸ Furthermore, BARF1-enriched EBV-specific CTL cultures can be successfully generated through minimal modification of the protocol currently used in clinic.⁴

In the present work, we described the generation and functional characterization of a new mouse mAb (3D4) that specifically recognizes a BARF1 minimal epitope (aa 28–35) located at the N-terminus of the molecule, in the region mediating malignant cell transformation and Bcl-2 upregulation.¹⁶ This characteristic differentiates the 3D4 mAb from other reported BARF1-specific antibodies, which preferentially target the C-terminus of the molecule.²⁷ More importantly, our results indicate that the 3D4 mAb recognizes the target antigen in its native conformation on the surface of tumor cell lines, as assessed by flow cytometry and functional tests. The detection of BARF1 protein in tumor specimens by immunohistochemistry was, however, frustrated by negative results, probably due to fixation-dependent conformation loss, and/or shedding of the molecule, as previously reported for other mAbs.¹² Our functional *in vitro* characterization showed that the 3D4 mAb is able to specifically and effectively mediate both CDC and ADCC activity against a panel of selected cell lines, whose entity paralleled the intensity of BARF1 expression. *In vivo*

biodistribution analyses disclosed a specific and long-lasting accumulation (up to 6 d) of the mAb on BARF1-expressing tumors, a critical pre-requisite for the therapeutic activity of a mAb. Moreover, our *in vivo* experiments demonstrated that the 3D4 mAb is able to exert a significant therapeutic activity in both loco-regional and disseminated *in vivo* mouse models of NPC and lymphoma. While NPC consistently express BARF1 along with the LMP1 oncoprotein, the chosen model for EBV-driven B-cell lymphoma (i.e., GRANTA-519 cell line) is peculiar considering that it is still unclear whether BARF1 can be expressed by latently infected lymphoma cells *in vivo*. Available data, however, support the rationale for the use of BARF1 targeting antibodies for the treatment of EBV⁺ lymphomas. In fact, BARF1-specific mAb therapy for lymphoma patients could be associated and synergize with lytic cycle inducers, such as doxorubicin.⁴ Albeit at different extents, tumor-bearing mice treated with anti-BARF1 mAb underwent a significant inhibition of tumor mass growth and experienced an improved survival, when compared with control groups. Noteworthy, in the GRANTA-519 cell line model, i.v. injection of anti-BARF1 antibody induced the complete regression of the mass in 2/10 of treated mice. The lack of any therapeutic effect shown in RAG^{-/-} γ -chain^{-/-} mice strongly indicates that the *in vivo* activity of the 3D4 mAb is mainly dependent on its ability to mediate ADCC, as also described for BARF1-specific antibodies from NPC patient sera.²¹ In addition to these direct effects on tumor cells, we could also expect an indirect antitumor activity. Indeed, unlike BARF1-specific CTL therapy that

can only targets antigens correctly presented at the cell surface in a MHC-restricted context, BАРF1-specific mAbs could also recognize and block soluble molecules, thus potentially hampering the mitogenic and immune-modulating activity of BАРF1 molecules shed in the tumor microenvironment. In particular, since the mAb recognizes an epitope near the aa involved in the interaction with hCSF-1 (aa 38–41¹⁸), it can be expected to influence this link by sterical hindrance and potentially relieve the inhibitory activity of BАРF1 on monocytes. This aspect is of particular interest in the case of NPC, where the infiltration with mononuclear cells correlates with patient survival.¹⁹ Unfortunately, in the mouse models used in the present study, this potential additional benefit cannot be appreciated, because BАРF1 does not interfere with the signaling mediated by mouse CSF1R and CSF1 molecules.¹⁸ Despite this limitation, these promising therapeutic results prompted us to broaden the use of this new tool to other EBV-related malignancies. Indeed, we obtained evidence that lymphoblastoid B cells (LCL, the *in vitro* model of PTLД) are also positively stained by our anti-BАРF1 3D4 mAb (data not shown).

Taken together, these data further substantiate the role of BАРF1 as a novel EBV-specific antigen suitable for immunotherapeutic approaches, and provide evidence indicating that the 3D4 anti-BАРF1 mAb can be a potent tool for the detection and treatment of several EBV-associated malignancies.

Materials and methods

Cell lines

The following human cell lines were used: GRANTA-519 (mantle B cell lymphoma, EBV⁺), C-666 (NPC, EBV⁺), BL-41 (Burkitt lymphoma, EBV⁻), BL-41 B95.8 (the same cell line infected with EBV), Raji (B lymphoblast-like cell, EBV⁺, but BАРF1⁻), Bjab (Burkitt lymphoma, EBV⁻), SNU-719 (GC, EBV⁺) and MKN-45 (GC, EBV⁻). All cell lines but SNU-719 and MKN-45 were cultured in RPMI-10 (RPMI 1640 medium, Euroclone, with 10% heat-inactivated Foetal Bovine Serum, FBS, Gibco, 10 mM HEPES Buffer, 1 mM Na Pyruvate, 2 mM Ultraglutamine, all from Lonza BioWhittaker, and 1% Antibiotic/antimycotic, Gibco). SNU-719 and MKN-45 were cultured in DMEM-10 (DMEM medium supplemented with the same additives).

Antibody production

BАРF1 sequence was analyzed using bioinformatic tools to select potential exposed epitopes that could be accessible for antibody binding. Three peptides derived from the main potentially immunogenic epitopes were designed for immunization, namely CVGKNDKEEAHGYYVSGYLSQ (BАРF1_{201–221}), CRMKLGETEVTKQEHLs (BАРF1_{104–120}) and RVTLSYWRRV (BАРF1_{28–38}), corresponding to aa sequence of BАРF1 protein 201–221, 104–120 and 28–38, respectively. An additional residue of cysteine was added at the N-terminal tail of peptide BАРF1_{28–38} to favor the conjugation to the carrier.

The peptides were synthesized at CRIBI (Padua University) by solid-phase technique using a multiple peptides synthesizer

(SyroII, MultiSynTech GmbH) on a pre-loaded Wang resin (100–200 mesh) (Novabiochem, Germany). The fluorenylmethoxycarbonyl (Fmoc) strategy was used throughout the peptide chain assembly, using O-(7-azabenzotriazol-1-yl)-N,N,N',N'-tetramethyluronium hexafluorophosphate (HATU) as coupling reagent.

Peptides were conjugated to maleimide-activated KLH (Keyhole Limpet Hemocyanin) by using Imject Maleimide Activated mCKLH Kit (Thermo Scientific), and used for mice immunizations. The anti-BАРF1 hybridoma was derived by fusing murine NS0 myeloma cells with the spleen cells from a BALB/c mouse that had been immunized once subcutaneously with 100 μ g of each KLH-conjugated peptide in Complete Freund Adjuvant (CFA, Sigma-Aldrich) and then twice with 100 μ g of each KLH-conjugated peptide in Incomplete Freund Adjuvant (IFA, Sigma-Aldrich). When necessary, additional immunizations were performed in IFA. Splenocytes from the immunized mouse were harvested and fused with NS0 myeloma cells using polyethyleneglycol (PEG, Sigma-Aldrich). Hybridoma clones were screened for BАРF1 reactivity by enzyme-linked immunosorbent assay (ELISA) and flow cytometry. For flow cytometry analysis, GRANTA-519 cells were stained with the supernatant of the clones, and subsequently with a secondary FITC anti-mouse antibody (Dako); finally, cells were analyzed using FACSCalibur (BD). Only those clones that gave a positive stain as assessed by flow cytometry were used for the subsequent experiments. Antibody recognition was assessed by Dot Blot. Briefly, we synthesized two peptides with a 4-aminoacid overlap, derived from the original 08/08_{28–39} peptide (used for all the experiments described here). The peptides and the original 08/08_{28–39}, 05/08_{201–221} and 06/08_{104–120} peptides were blotted on a PVDF membrane (Millipore) and stained with the anti-BАРF1 mAb. The positive signal was evaluated by chemiluminescence using a ChemiDoc XRS instrument and QuantityOne (vers. 4.6) software (both from BioRad).

Flow cytometry analysis of BАРF1 staining

BАРF1-negative (BJAB, RAJI, BL-41) and -positive (GRANTA-519, C-666, BL-41 B95.8 and SNU-719) cell lines were stained with the anti-BАРF1 mAb. Moreover, we generated a BАРF1-transduced cell line by transducing MKN-45 cells with a BАРF-1 retrovirus.⁴

Evaluation of complement-dependent cytotoxicity (CDC)

Target cells (6×10^5 GRANTA-519, C-666, BL-41, BL-41 B95.8 cells and SNU-719) were labeled with 100 μ Ci Na₂⁵¹CrO₄ (PerkinElmer). After addition of 1 μ g anti-BАРF1 mAb, cells were incubated in 200 μ L RPMI-25% Human Serum (non-heat inactivated; Lonza), for 1 h at 37°C. Negative controls (or spontaneous release) were cells without mAb, while for positive control (maximum release) 100 μ L Triton 5% (Sigma-Aldrich) were added. Supernatant radioactivity was evaluated by using a γ -ray counter (Cobra Gamma Counting System, Packard Instrument Company). The percentage of specific cell lysis was calculated as follows: $100 \times [(A - C) / (B - C)]$, where A represents an absorbance obtained with

test serum (experimental release), *C* and *B* the minimum (heat-inactivated serum) and maximum release (with Triton 5%), respectively.

Evaluation of antibody-dependent cell-mediated cytotoxicity (ADCC)

ADCC was performed following Calcein-AM (Invitrogen) protocol. Briefly, 1×10^6 target cells were re-suspended in 1 mL Hank's Balanced Salt Solution added with 5% FBS (HBSS-FBS) and labeled with 7.5 μL of Calcein-AM 1 mg/mL for 30 min at 37 °C. Cells were then labeled with anti-BARF1 mAb at a concentration of 20 $\mu\text{g}/\text{mL}$, 10 $\mu\text{g}/\text{mL}$ and 5 $\mu\text{g}/\text{mL}$, while negative controls were performed with HBSS-FBS only. As a positive control, target cells were lysed with Triton 5%. Cells were seeded, and effector cells were added: freshly thawed PBMC from healthy donors were seeded at different effector-target ratios (300:1, 150:1 and 75:1) for 4 h at 37°C, then 100 μL of supernatant were collected and seeded on a 96-well Black OptiPlate (Nunc). After 15 min at RT, the plate was read at 485 nm using Victor X3 Multilabel Plate reader. Lysis percentage (% Lys) was calculated as in CDC.

Mice

In vivo experiments involved 6- to 8-week-old SCID, RAG^{-/-} γ -chain^{-/-} and BALB/c mice (Charles River Laboratories), which were housed in our Specific Pathogen Free (SPF) animal facility. Procedures involving animals and their care were conducted according to institutional guidelines that comply with national and international laws and policies (D.L. 116/92 and subsequent implementing circulars), and the experimental protocol (project ID: 2/2012) was approved by the local Ethical Committee of Padua University (CEASA). During *in vivo* experiments, animals in all experimental groups were examined daily for a decrease in physical activity and other signs of disease; severely ill animals (weight loss exceeding 15%, lethargy, ruffled hair, low temperature) were killed by carbon dioxide overdose.

Biodistribution analysis

To study the antibody biodistribution, anti-BARF1 mAb was conjugated to Alexa 680 using SAIKI Rapid Antibody Labeling Kit (Invitrogen), and following the manufacturer's indications. SCID mice were injected s.c. on one flank with an EBV-negative cell line (MKN-45) and on the opposite one with a BARF1-positive cell line (C-666 or BARF1-transduced MKN-45). As soon as both tumors became palpable, 100 μg Alexa-680 anti-BARF1 antibody were injected via tail vein in the anaesthetized animal, and the fluorescence signal was analyzed by total body scanning every 24 h using an MX2 apparatus (ART, Canada), as previously reported.^{25, 29}

Assessment of therapeutic efficacy

Six-to-eight-week-old SCID and RAG^{-/-} γ -chain^{-/-} mice were injected s.c. with 5×10^6 C-666 or GRANTA-519 cells. Mice were then divided into untreated and treated groups,

which received PBS or 1 mg anti-BARF1 mAb (5 i.p. injections of 0.2 mL each, one every 2 d), respectively, starting from day 10 or 14 after C-666 or GRANTA-519 tumor injection, respectively. Tumor masses were evaluated every 2 d by measuring maximum and minimum diameter, and tumor volume was calculated applying the formula: $(d \times d \times D)/2$, where *d* and *D* are the minimum and maximum diameters, respectively. Moreover, tumor cell lines were transduced with a firefly luciferase-encoding lentiviral (LV-LUX) vector as described previously.³⁰ In different experiments, SCID mice were injected i.v. with 3×10^6 Luciferase-transduced C-666 or GRANTA-519 cells. Then, treated mice received from day 10 (C-666) or 14 (GRANTA-519) and weekly thereafter 0.3 mg/mouse of anti-BARF1 mAb. Bioluminescence (BLI) images were acquired at different time points after *in vivo* cell injection using the IVIS Lumina II Imaging System (PerkinElmer). Ten minutes before each imaging session, animals were anaesthetized with isoflurane/oxygen and administered i.p. with 150 mg/kg of D-luciferin (PerkinElmer) in Dulbecco's Phosphate-Buffered Saline (DPBS), and the signal intensity was measured as radiance (photon/sec) using the LivingImage software 3.2 (PerkinElmer). Tumor growth and response to therapy were monitored by BLI and by recording survival.

Statistical analysis

Both for the tumor growth and the BLI analysis, ANOVA for repeated measures test was performed between control and treated group, using MedCalc, version 9.4.2.0. Survival diagrams and analysis of the survival data (using Kaplan-Meier test) were performed with the same statistical software.




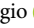
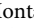




Disclosure of potential conflicts of interest

No potential conflicts of interest were disclosed.

Funding

This work was partly supported by grants from the Italian Association for Cancer Research (AIRC, IG-17035 and Special Program Molecular Clinical Oncology 5 per mille ID 10016), and Progetto di Ricerca di Ateneo 2015, University of Padova, to AR.

ORCID

Riccardo Turrini  <http://orcid.org/0000-0003-0133-7492>
 Debora Martorelli  <http://orcid.org/0000-0001-7385-3571>
 Damiana Antonia Faè  <http://orcid.org/0000-0003-3660-0502>
 Roberta Sommaggio  <http://orcid.org/0000-0002-5682-5867>
 Isabella Monia Montagner  <http://orcid.org/0000-0002-5778-2221>
 Oriano Marin  <http://orcid.org/0000-0002-6175-4039>
 Paola Zanovello  <http://orcid.org/0000-0003-0740-4043>
 Riccardo Dolcetti  <http://orcid.org/0000-0003-1625-9853>
 Antonio Rosato  <http://orcid.org/0000-0002-5263-8386>

References

1. Young LS, Rickinson AB. Epstein-Barr virus: 40 years on. *Nat Rev Cancer* 2004; 4:757-68; PMID:15510157; <http://dx.doi.org/10.1038/nrc1452>
2. Merlo A, Turrini R, Dolcetti R, Martorelli D, Muraro E, Comoli P, Rosato A. The interplay between Epstein-Barr virus and the immune

- system: a rationale for adoptive cell therapy of EBV-related disorders. *Haematologica* 2010; 95:1769-77; PMID:20421267; <http://dx.doi.org/10.3324/haematol.2010.023689>
3. Martorelli D, Houali K, Caggiari L, Vaccher E, Barzan L, Franchin G, Gloghini A, Pavan A, Tedeschi RM, De Re V et al. Spontaneous T cell responses to Epstein-Barr virus-encoded BARTF1 protein and derived peptides in patients with nasopharyngeal carcinoma: bases for improved immunotherapy. *Int J Cancer* 2008; 123:1100-7; PMID:18546263; <http://dx.doi.org/10.1002/ijc.23621>
 4. Fae DA, Martorelli D, Mastorci K, Muraro E, Dal Col J, Franchin G, Barzan L, Comaro E, Vaccher E, Rosato A et al. Broadening specificity and enhancing cytotoxicity of adoptive T Cells for Nasopharyngeal Carcinoma immunotherapy. *Cancer Immunol Res* 2016; 4:431-40; PMID:27009165; <http://dx.doi.org/10.1158/2326-6066.CIR-15-0108>
 5. Decaussin G, Sbih-Lammali F, de Turenne-Tessier M, Bouguermouh A, Ooka T. Expression of BARTF1 gene encoded by Epstein-Barr virus in nasopharyngeal carcinoma biopsies. *Cancer Res* 2000; 60:5584-8; PMID:11034107
 6. Seto E, Yang L, Middeldorp J, Sheen TS, Chen JY, Fukayama M, Eizuru Y, Ooka T, Takada K. Epstein-Barr virus (EBV)-encoded BARTF1 gene is expressed in nasopharyngeal carcinoma and EBV-associated gastric carcinoma tissues in the absence of lytic gene expression. *J Med Virol* 2005; 76:82-8; PMID:15778977; <http://dx.doi.org/10.1002/jmv.20327>
 7. zur Hausen A, Brink AA, Craanen ME, Middeldorp JM, Meijer CJ, van den Brule AJ. Unique transcription pattern of Epstein-Barr virus (EBV) in EBV-carrying gastric adenocarcinomas: expression of the transforming BARTF1 gene. *Cancer Res* 2000; 60:2745-8; PMID:10825150
 8. Griffin BE, Karran L. immortalization of monkey epithelial cells by specific fragments of Epstein-Barr virus DNA. *Nature* 1984; 309:78-82; PMID:6325929
 9. Karran L, Teo CG, King D, Hitt MM, Gao YN, Wedderburn N, Griffin BE. Establishment of immortalized primate epithelial cells with subgenomic EBV DNA. *Int J Cancer* 1990; 45:763-72; PMID:2157679
 10. Wei MX, Moulin JC, Decaussin G, Berger F, Ooka T. Expression and tumorigenicity of the Epstein-Barr virus BARTF1 gene in human Louckes B-lymphocyte cell line. *Cancer Res* 1994; 54:1843-8; PMID:8137299
 11. Wei MX, Ooka T. A transforming function of the BARTF1 gene encoded by Epstein-Barr virus. *Embo J* 1989; 8:2897-903; PMID:2555151
 12. Hoebe EK, Le Large TY, Greijer AE, Middeldorp JM. BamHI-A rightward frame 1, an Epstein-Barr virus-encoded oncogene and immune modulator. *Rev Med Virol* 2013; 23:367-83; PMID:23996634; <http://dx.doi.org/10.1002/rmv.1758>
 13. Houali K, Wang X, Shimizu Y, Djennaoui D, Nicholls J, Fiorini S, Bouguermouh A, Ooka T. A new diagnostic marker for secreted Epstein-Barr virus encoded LMP1 and BARTF1 oncoproteins in the serum and saliva of patients with nasopharyngeal carcinoma. *Clin Cancer Res* 2007; 13:4993-5000; PMID:17785549; <http://dx.doi.org/10.1158/1078-0432.CCR-06-2945>
 14. Sall A, Caserta S, Jolicoeur P, Franqueville L, de Turenne-Tessier M, Ooka T. Mitogenic activity of Epstein-Barr virus-encoded BARTF1 protein. *Oncogene* 2004; 23:4938-44; PMID:15064715; <http://dx.doi.org/10.1038/sj.onc.1207607>
 15. Chang MS, Kim DH, Roh JK, Middeldorp JM, Kim YS, Kim S, Han S, Kim CW, Lee BL, Kim Wh et al. Epstein-Barr virus-encoded BARTF1 promotes proliferation of gastric carcinoma cells through regulation of NF-kappaB. *J Virol* 2013; 87:10515-23; PMID:23824821; <http://dx.doi.org/10.1128/JVI.00955-13>
 16. Sheng W, Decaussin G, Sumner S, Ooka T. N-terminal domain of BARTF1 gene encoded by Epstein-Barr virus is essential for malignant transformation of rodent fibroblasts and activation of BCL-2. *Oncogene* 2001; 20:1176-85; PMID:11313861; <http://dx.doi.org/10.1038/sj.onc.1204217>
 17. Kim DH, Chang MS, Yoon CJ, Middeldorp JM, Martinez OM, Byeon SJ, Rha SY, Kim SH, Kim YS, Woo JH. Epstein-Barr virus BARTF1-induced NFkappaB/miR-146a/SMAD4 alterations in stomach cancer cells. *Oncotarget* 2016; 7:82213-27; PMID:27438138; <http://dx.doi.org/10.18632/oncotarget.10511>
 18. Elegheert J, Bracke N, Pouliot P, Gutsche I, Shkumatov AV, Tarbouriech N, Verstraete K, Bekaert A, Burmeister WP, Svergun DI et al. Allosteric competitive inactivation of hematopoietic CSF-1 signaling by the viral decoy receptor BARTF1. *Nature Struct Mol Biol* 2012; 19:938-47; PMID:22902366; <http://dx.doi.org/10.1038/nsmb.2367>
 19. Hoebe EK, Le Large TY, Tarbouriech N, Oosterhoff D, De Gruijl TD, Middeldorp JM, Greijer AE. Epstein-Barr virus-encoded BARTF1 protein is a decoy receptor for macrophage colony stimulating factor and interferes with macrophage differentiation and activation. *Viral Immunol* 2012; 25:461-70; PMID:23061794; <http://dx.doi.org/10.1089/vim.2012.0034>
 20. Cohen JI, Lekstrom K. Epstein-Barr virus BARTF1 protein is dispensable for B-cell transformation and inhibits alpha interferon secretion from mononuclear cells. *J Virol* 1999; 73:7627-32; PMID:10438853
 21. Tanner JE, Wei MX, Alfieri C, Ahmad A, Taylor P, Ooka T, Menezes J. Antibody and antibody-dependent cellular cytotoxicity responses against the BamHI A rightward open-reading frame-1 protein of Epstein-Barr virus (EBV) in EBV-associated disorders. *J Infect Dis* 1997; 175:38-46; PMID:8985194
 22. Strockbine LD, Cohen JI, Farrah T, Lyman SD, Wagener F, DuBose RF, Armitage RJ, Spriggs MK. The Epstein-Barr virus BARTF1 gene encodes a novel, soluble colony-stimulating factor-1 receptor. *J Virol* 1998; 72:4015-21; PMID:9557689
 23. Hatfull G, Bankier AT, Barrell BG, Farrell PJ. Sequence analysis of Raji Epstein-Barr virus DNA. *Virology* 1988; 164:334-40; PMID:2835854
 24. Fiorini S, Ooka T. Secretion of Epstein-Barr virus-encoded BARTF1 oncoprotein from latently infected B cells. *Virology* 2008; 370:5-70; PMID:18533018; <http://dx.doi.org/10.1186/1743-422X-5-70>
 25. Frigerio B, Fracasso G, Luison E, Cingarlini S, Mortarino M, Coliva A, Seregni E, Bombardieri E, Zuccolotto G, Rosato A et al. A single-chain fragment against prostate specific membrane antigen as a tool to build theranostic reagents for prostate cancer. *Eur J Cancer (Oxford, England : 1990)* 2013; 49:2223-32; PMID:23433847; <http://dx.doi.org/10.1016/j.ejca.2013.01.024>
 26. Teo EC, Chew Y, Phipps C. A review of monoclonal antibody therapies in lymphoma. *Crit Rev Oncol Hematol* 2016; 97:72-84; PMID:26318093; <http://dx.doi.org/10.1016/j.critrevonc.2015.08.014>
 27. Hoebe EK, Hutajulu SH, van Beek J, Stevens SJ, Paramita DK, Greijer AE, Middeldorp JM. Purified hexameric Epstein-Barr virus-encoded BARTF1 protein for measuring anti-BARTF1 antibody responses in nasopharyngeal carcinoma patients. *Clin Vaccine Immunol : CVI* 2011; 18:298-304; PMID:21123521; <http://dx.doi.org/10.1128/0193-10>
 28. Pasini E, Caggiari L, Dal Maso L, Martorelli D, Guidoboni M, Vaccher E, Barzan L, Franchin G, Gloghini A, De Re V et al. Undifferentiated nasopharyngeal carcinoma from a nonendemic area: protective role of HLA allele products presenting conserved EBV epitopes. *Int J Cancer* 2009; 125:1358-64; PMID:19536817; <http://dx.doi.org/10.1002/ijc.24515>
 29. Bobisse S, Rondina M, Merlo A, Tisato V, Mandruzzato S, Amendola M, Naldini L, Willemsen RA, Debets R, Zanovello P et al. Reprogramming T lymphocytes for melanoma adoptive immunotherapy by T-cell receptor gene transfer with lentiviral vectors. *Cancer Res* 2009; 69:9385-94; PMID:19996290; <http://dx.doi.org/10.1158/0008-5472.CAN-09-0494>
 30. Keyaerts M, Verschuere J, Bos TJ, Tchouate-Gaikam LO, Peleman C, Breckpot K et al. Dynamic bioluminescence imaging for quantitative tumour burden assessment using IV or IP administration of D-luciferin: effect on intensity, time kinetics and repeatability of photon emission. *Eur J Nucl Med Mol I* 2008; 35:999-1007; PMID:18180921; <http://dx.doi.org/10.1007/s00259-007-0664-2>